JOURNAL OF MATERIALS RESEARCH AND TECHNOLOGY 2021;15:4309–4316

Available online at www.sciencedirect.com

jmr&t Journal of Materials Research and Technology

journal homepage: www.elsevier.com/locate/jmrt

Original Article

The hygroscopicity of moso bamboo (*Phyllostachys edulis*) with a gradient fiber structure

Xin Wei [a,b], *Ge Wang* [a,*], *Lee Miller Smith* [c], *Huan Jiang* [a,b]

[a] *International Center for Bamboo and Rattan, Beijing 100102, PR China*
[b] *Key Laboratory of National Forestry and Grassland Administration/Beijing for Bamboo & Rattan Science and Technology, Beijing 100102, PR China*
[c] *Mechanical Engineering, University of North Texas (UNT), Denton, TX 76203, USA*

ARTICLE INFO

Article history:
Received 30 August 2021
Accepted 9 October 2021
Available online 15 October 2021

Keywords:
Hygroscopicity
Bamboo
Gradient fiber structures
Mesopore structures
Haillwood–Horrobin (H–H) model

ABSTRACT

Bamboo is a functionally graded material with natural hygroscopicity, and the study of the response of its cell structure to humidity will help expand its use in textiles and engineering structures. For this purpose, in this study, the hygroscopicity of moso bamboo (*Phyllostachys edulis*) with a gradient fiber structure was assessed by a dynamic vapor sorption (DVS) apparatus and fitted with a Haillwood–Horrobin (H–H) model. The effects of the chemical composition, gradient fiber structure, and mesopore structure of the bamboo were also investigated. The results demonstrate that the hygroscopicity of bamboo gradually increases from the outer to the inner layer along the thickness of the culm wall, which is related to the gradient distribution of the fibers. Based on the H–H model, the hygroscopic mechanism of bamboo was determined as follows. The primary sites derived from amorphous cellulose and hemicellulose act in the low-humidity stage, while the mesopores provide a huge specific surface area (153–132 m^2/g), which helps condense water vapor in high-humidity environments. Based on numerical modeling, the hygroscopic ratio of parenchyma cells and fibers was found to be 13:5, indicating that parenchyma cells contribute more to the overall hygroscopicity of moso bamboo. Moreover, the contribution of cellulose to hygroscopicity was found to become gradually higher than that of hemicellulose from the inner to the outer layer due to the increase of the amorphous area (–OH groups). The structure–function relationships between the chemical composition, multi-scale structure, and hygroscopicity identified in this study provide a theoretical basis for bamboo drying and storage technology, as well as the processing and application of bamboo fiber-based composites.

* Corresponding author.
E-mail address: wangge@icbr.ac.cn (G. Wang).

https://doi.org/10.1016/j.jmrt.2021.10.038

1. Introduction

Bamboo is a large collection of herbaceous species with lignified stems. Due to its rich sources, excellent mechanical performance, and suitable colors, bamboo has been widely used in decorative, construction, and engineering applications [1–3]. When applied in various dynamic environments, bamboo regulates the humidity comfort by allowing sorption from indoor air [4]. As the equilibrium moisture content (EMC) increases, bamboo also exhibits certain properties of deterioration, such as dimensional instability, biodegradation, and decreased strength [5]. This greatly limits the application of bamboo, especially in hot and humid environments. Consequently, it is important to thoroughly study the hygroscopic response of bamboo to understand the conflict between its performance and environmental humidity regulation.

The hygroscopicity of bamboo is primarily influenced by its chemical composition, cell structure, and cell distribution [6–8]. The chemical composition and morphological structure of bamboo cells vary with the bamboo species, age, and location (e.g., stalks and roots), which result in different hygroscopicity [4,9]. Chen et al. [10] found that the inner layer of bamboo exhibits the highest EMC due to its high concentration of parenchyma cells. As an optimized functionally graded material (FGM), derived from varying distributions of the fibers and parenchyma cells in the bamboo culm along the radial direction, the gradient distribution of fibers enhances the mechanical properties of bamboo (e.g., less stress concentration and increased bonding strength) [7]. However, the effect of the hygroscopicity of bamboo with a gradient fiber structure on its mechanical properties is not deeply understood, and the contributions of parenchyma cells and fibers to the overall hygroscopicity of the bamboo have not been quantitatively investigated.

The pore structure in the bamboo cell walls is also one of the main factors affecting the hygroscopicity of bamboo, including its porosity and inner surface area. Krause et al. [11] found that bamboo has considerable multi-scale pores, primarily vessels, pores, and lumina, with a porosity of 27%–40% from the inner to the outer layers of the bamboo culm. Zhang et al. [12] demonstrated that the hygroscopicity of fibers is lower than that of parenchyma cells at the same relative humidity, which is associated with the larger cell cavities and specific surface of parenchyma cells. When water molecules are adsorbed on the surface of bamboo cell walls, they penetrate the inner surface as well as the pores, and even the molecular chains within the cell walls. Water penetration will specially occur within mesopores, which can help to generate capillary condensate to increase the amount of water content in high-humidity environments. This is similar to other lignocellulosic materials [13] and inorganic porous shale [14]. Therefore, the study of the mesopore structure in bamboo is of great significance for the understanding of the water molecule sorption in bamboo cell walls.

This work aims to reveal the hygroscopic response of moso bamboo (*Phyllostachys edulis*) with a gradient fiber structure via the use of results from the dynamic vapor sorption (DVS) technique fitted with a Haillwood–Horrobin (H–H) model. By analyzing the response, the effects of the chemical composition, gradient fiber structure, and mesopore structure are observed. The structure–function relationships between the chemical composition, multi-scale structure, and hygroscopicity generated in this study provide a theoretical basis for bamboo drying and storage technology, as well as the processing and application of bamboo fiber-based composites.

2. Materials and methods

2.1. Sample preparation

A four-year-old mature moso bamboo was collected from a bamboo plantation located in Fujian Province, China, and was selected as the raw material for use in this study. The bamboo culm (collected from 2 m above the ground to ensure stable physical and chemical performance) was processed into bamboo blocks ($10 \times 10 \times 10$ mm^3) by removing the innermost and outermost layers (Fig. 1), and then was divided into 3 slices from the inner (IB), middle (MB), and outer (OB) bamboo layers along the thickness of the culm.

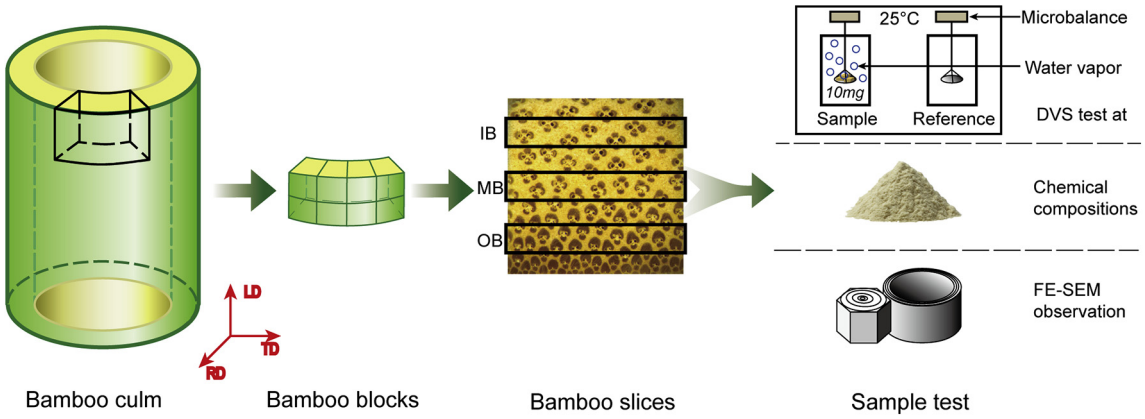

Fig. 1 – Bamboo samples preparation for dynamic water vapor sorption test, chemical compositions analysis and SEM observation.

2.2. Dynamic water vapor sorption (DVS) test

The water vapor sorption behavior of all samples was tested using a DVS Adventure analyzer (Surface Measurement Systems, UK) (Fig. 1). About 10 mg of samples were placed on a microbalance with a mass resolution of 0.1 μg in a sample chamber after being dried at 103 °C. The DVS test was carried out at a constant temperature of 25 ± 0.1 °C while increasing the relative humidity (RH) from 0% to 95% at increments of 10%, and then decreasing the RH back to 0% at the same rate.

2.3. Sorption models

The well-documented studies on the water vapor adsorption of organic or inorganic porous materials can be broadly divided into two categories [15,16], namely those considering monolayer adsorption theory based on the Langmuir model and multilayer adsorption based on the Brunauer–Emmett–Teller (BET) model. Following the multilayer theory, the Haillwood–Horrobin (H–H) model [17] is applied to depict the multilayer adsorption behavior of water vapor on plant fiber materials and fiber-based composites [4,18–22]. Bamboo is a typical lignocellulosic material with multi-scale pores. The total adsorption capacity of the surfaces of the hydrophilic pores on bamboo changes with the environmental humidity, and can be fitted to the H–H model as follows:

$$EMC = Mo + Mu = 1800/W^{*}K_1K_2RH/(100 + K_1K_2RH) + 1800/W^{*}K_2RH/(100 - K_2RH) \quad (1)$$

where EMC (%) is the EMC of bamboo at a certain environmental RH (%), Mo (%) is the monolayer adsorbed water content, Mu (%) is the multilayer adsorbed water content, W (g/mol) is the molecular weight of the cell wall polymer per adsorption site, which is determined numerically, and K_1 and K_2, are equilibrium constants related to adsorption.

Considering the gradient behavior of the hygroscopicity of bamboo caused by the gradient distribution of fibers and parenchyma cells, a numerical model is introduced to take into account the respective adsorption capacities of fibers and parenchyma cells [3]:

$$EMCmax = EMC_f + EMC_p = A_fV_f + A_p(1 - V_f) = (A_f - A_p)V_f + A_p \quad (2)$$

where $EMCmax$ (%) is the EMC at 95% RH of the bamboo layer with fiber volume fraction V_f, EMC_f and EMC_p (%) are the adsorption capacities of fibers and parenchyma cells, respectively, and A_f and A_p (%) are the adsorption capacities per gram of fibers and parenchyma cells, respectively.

2.4. SEM observation

The bamboo samples were cut along the transverse and longitudinal directions, coated with a thin layer of platinum, and then observed by a field emission scanning electron microscope (FE-SEM, XL30, FEI, USA) at 7.0 kV.

2.5. Chemical composition analysis

The samples were milled into fine powders separated by a 60-mesh sieve, and were then dried at 103 °C until they reached a constant weight (Fig. 1). All samples were subjected to phenyl alcohol extraction (1/2, v/v) in a Soxhlet apparatus for 6 h. In accordance with Dixon et al. [23], the extracted samples were used to determine the holocellulose content by removing lignin with sodium chlorite solution ($NaClO_2$, 17.5t% w/w), and hemicellulose (polypentose) was obtained by washing it with sodium hydroxide solution (NaOH, 10% w/w). The acid-insoluble (Klason) lignin was obtained according to the ASTM D1106-1996 standard (2013) [24].

3. Results and discussion

3.1. Dynamic hygroscopic behavior

The changes in the EMC of the IB, MB, and OB samples at different RH were plotted, as presented in Fig. 2A. For all curves, the increasing (adsorption) and decreasing (desorption) sections formed a closed double "S," which reflects a typical type II isotherm according to Brunauer et al. [16]. In general, each adsorption isotherm can be divided into 3

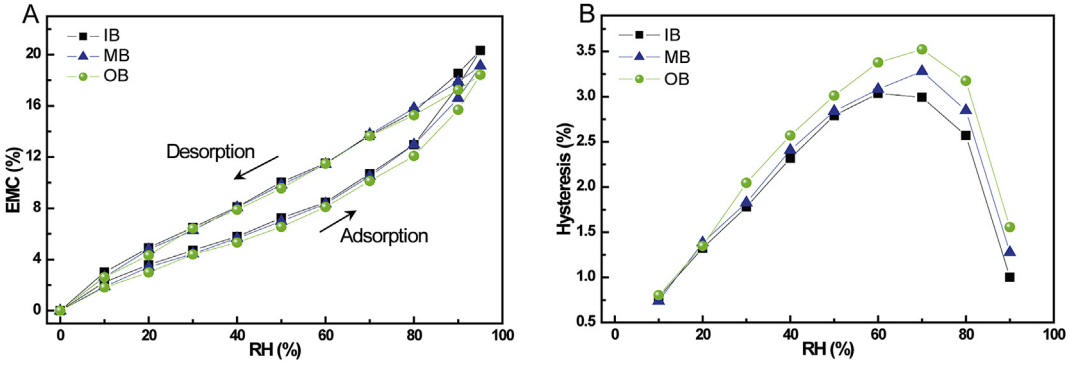

Fig. 2 – The hygroscopic behavior at 25 °C of bamboo with its gradient fibbers structure. A. The equilibrium moisture content (EMC) and B. hysteresis of the inner, middle and outer bamboos (IB, MB, and OB) plotted as a function of environmental RH.

Table 1 – Fitting parameters obtained from the H–H model for the IB, MB, and OB.

	Adsorption								Desorption			
	1/W ($\times 10^{-3}$ mol/g)	K_1	K_2	R^2	Momax (%)	Mumax (%)	EMCmax (%)	S (m^2/g)	W (g/mol)	K_1	K_2	R^2
IB	2.91	6.27	0.79	0.9995	4.32	16.06	20.38	153	197	5.29	0.63	0.9988
MB	2.75	5.82	0.79	0.9985	4.03	15.16	19.20	143	149	3.48	0.52	0.9997
OB	2.51	6.23	0.80	0.9992	3.74	14.68	18.42	132	131	3.10	0.46	0.9994

stages. In the low-RH range (<20%) the EMC increased rapidly. With the increase of RH, the slope of the isotherms slowed down. When the RH was greater than 80%, the EMC increased sharply to the maximum value. As a result, the EMC of the IB reached a maximum value of 20.38% at an RH of 95% or higher, and was higher than those of the MB and OB samples; this is related to the gradient fiber structure of bamboo from the inner to the outer layer of the culm.

Hysteresis, which is defined as the difference in EMC between desorption and adsorption at the same RH, can be used to describe the incomplete reversibility of sorption when water molecules enter and exit the cell wall matrix in plant fibers [21]. All bamboo samples exhibited the hysteresis phenomenon throughout the entire investigated RH range, and the hysteresis curves reached peaks values at RH = 70% before they began to fall (Fig. 2B). The hysteresis in the OB sample was higher than that in the MB and IB samples, which is due to the high fiber content in the OB.

3.2. *Fitting model and hygroscopic mechanism*

The experimental sorption data of the IB, MB, and OB samples were fitted to an H–H model (Eq. (1)) with an RH range from 0% to 95%. The fitting parameters in the theoretical model (i.e., 1/W, K_1, and K_2) revealed high fitting accuracy ($R^2 > 0.998$) for all samples, which indicates that the H–H model can describe the experimental sorption data (Table 1). By introducing the parameters K_1 and K_2 into the H–H model, the typical fitting curves of the EMC, monolayer (*Mo*), and multilayer (*Mu*) adsorption isotherms as a function of RH were obtained, as exhibited in Fig. 3A. In the low-RH range (0 < RH < 20%), the fitting curve increased sharply due to the monolayer on the primary active sites. As the RH increased, the multilayer absorbed on secondary sites by H-bonds and van der Waals forces began to dominate the adsorption process by forming a large number of water clusters, which resulted in the rise of the curve, especially when RH > 60% (Fig. 3B). The primary and secondary adsorption sites had different contribution rates in environments with different humidity.

The adsorption sites were found to be related to the content of hygroscopic chemical components. The main hygroscopic chemical components in bamboo include cellulose, hemicellulose, and lignin, and the compositions of these components differ between the IB, MB, and OB layers (Fig. 4). Among these components, hemicellulose is generally considered to be more hygroscopic than cellulose and lignin at the same weight, as the main chain and side chains of the full amorphous structure contain large numbers of hydrophilic groups (–OH, C=O) [4]. However, the cellulose content of bamboo (43.84–46.63%) is much higher than the hemicellulose content (18.95–21.82%). It is conceivable that the contributions of cellulose and hemicellulose to the total hygroscopicity of bamboo should be judged based on the contents of amorphous cellulose and hemicellulose, as water cannot enter the cellulose crystal area. Zhang et al. [25] determined the crystallinity of bamboo cellulose nanofibrils (CNFs) to be 43.6%, i.e., the ratio of crystal and amorphous areas in the cellulose is about 1:1. For the IB layer, the content of amorphous cellulose (21.92%) was found to be close to that of hemicellulose (21.28%), which implies that the two make approximately equivalent contributions to hygroscopicity [26]. For the OB layer, the contribution of amorphous cellulose (23.31%) was found to be greater than that of hemicellulose (18.95%).

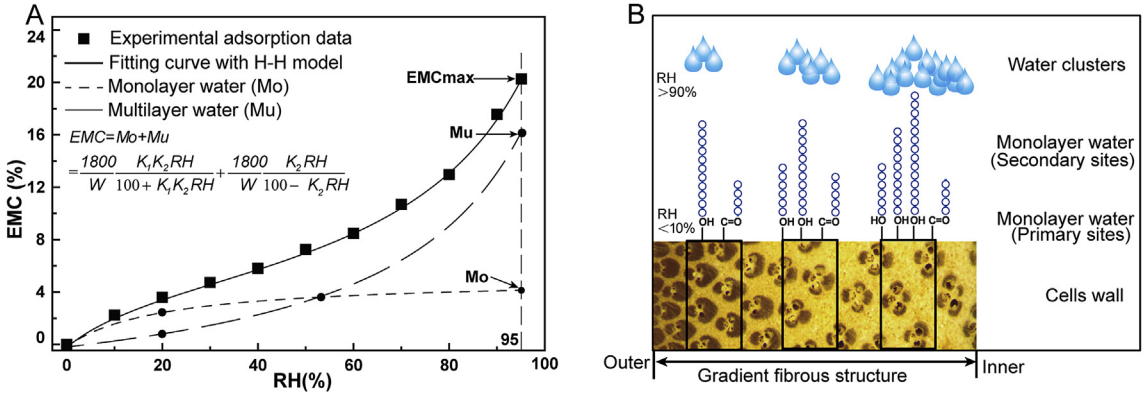

Fig. 3 – The hygroscopic mechanism of bamboo from the H–H model. A. The equilibrium moisture content (EMC), monolayer (Mo) and multilayer (Mu) adsorption curves at 25 °C as a function of RH. B. The schematic diagram of hygroscopic mechanism of bamboo with a gradient fiber structure.

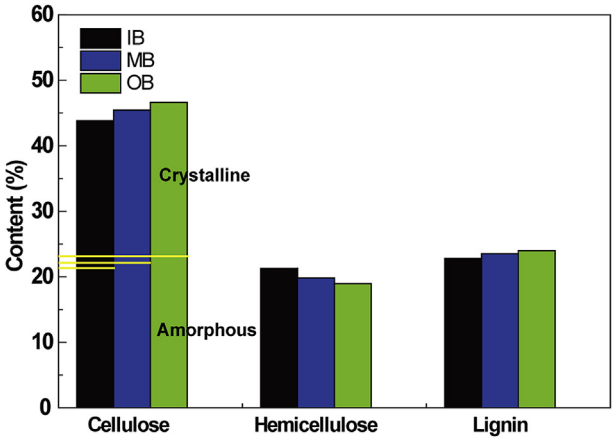

Fig. 4 – Chemical compositions related to hygroscopicity for IB, MB, and OB.

3.3. *Gradient fiber structure*

The hygroscopic behavior exhibited by the bamboo, especially the *EMC*max value at 95% RH from the IB to the OB layer, can be primarily attributed to the gradient distribution of fibers and parenchyma cells (Fig. 5A). It is already known that, compared to fibers (10%) [10], parenchyma cells have a significantly higher EMC (20%) [12], and any variation in their volume fractions can affect the overall hygroscopicity of bamboo.

By fitting Eq. (2) to the test values of *EMC*max derived for the IB, MB, and OB layers, it was found that the *EMC*max and fiber volume fraction (V_f) exhibited a steep linear inverse relationship with a strong correlation ($R^2 = 0.8448$) (Fig. 5B). The theoretical *EMC*max values of parenchyma cells and fibers were determined to be 20.1% and 12.9%, respectively. The contribution ratio of parenchyma cells to fibers (A_p:A_f) was determined to be about 13:5 from the bamboo slices, which was higher than the test results (about 6:5) of powder separated by hand [12]. It has been proven that a large sample size affects the rate and capacity of moisture adsorption, and delays the diffusion of adsorbed water to the internal fiber cells [27], which ultimately causes differences between bamboo slices and powder.

Based on the hygroscopic behavior and mechanism of bamboo with a gradient fiber structure, bamboo strips sampled from different parts along the thickness of the culm should be dried and stored at different temperatures and humidity conditions because the inner layer more easily adsorbs and desorbs moisture. In addition, in the processing of a new type of bamboo fiber-based composite material, namely reconstituted bamboo, the raw material fiber bundles with low moisture adsorption are obtained via a rolling and brooming process by removing most of the highly hygroscopic parenchyma cells in the bamboo strips, which helps to increase the bond strength of the fiber/resin interface.

3.4. *Mesopore structures*

The multi-scale pore structure of bamboo can be classified as cell pores, cell wall pores, and intermolecular chain pores within cell walls (Fig. 6). Macropores refer to various types of tubular pores in bamboo cells with diameters greater than 50 nm or even tens of micrometers, and include intercellular pores (cells corners) or canals, cell (fibers, parenchyma cells, and vessels) cavity pores, and pits (Fig. 6A–D) [28,29]. Mesopores refer to slit-like pores in the cell walls, such as microfibril gaps in the dry or wet state, which are mainly due to the formation of cellulose microfibrils filled with lignin and hemicellulose (Fig. 6E) [30]. Furthermore, the gaps between the cellulose intermolecular chains within cell walls refer to micropores, which are smaller than 2 nm in the Meyer–Misch models (Fig. 6F).

These multi-scale pores provide a large surface space available for secondary reaction sites for water molecules. Among these pores, mesopores can condense water molecules adsorbed on the sites via capillary force in a high-RH environment, so their structures were further analyzed. Assuming that monolayer water molecules were fully adsorbed on the primary active sites of the bamboo surface, according to the H–H model, the specific surface area (*S*) of mesopores was calculated as follows [31]:

$$S = N^{*}A_{w}Mo/M \quad (3)$$

where *Mo* is the monolayer adsorption water at 100% RH (here, *Mo*max was adopted), *N* is Avogadro's number, A_w is the

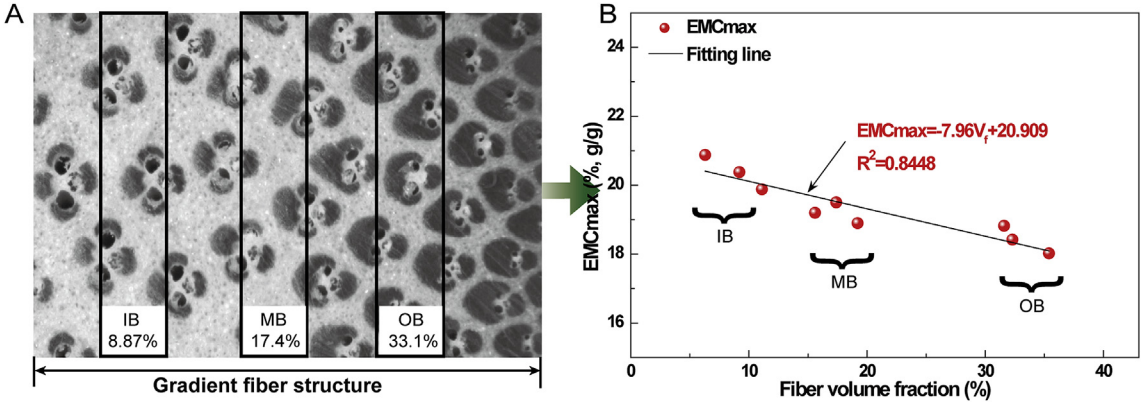

Fig. 5 – The A. gradient fiber structure of bamboo creating a variable hygroscopicity (EMCmax at 25 °C) from the inner to outer layer fitted by B. a numerical model.

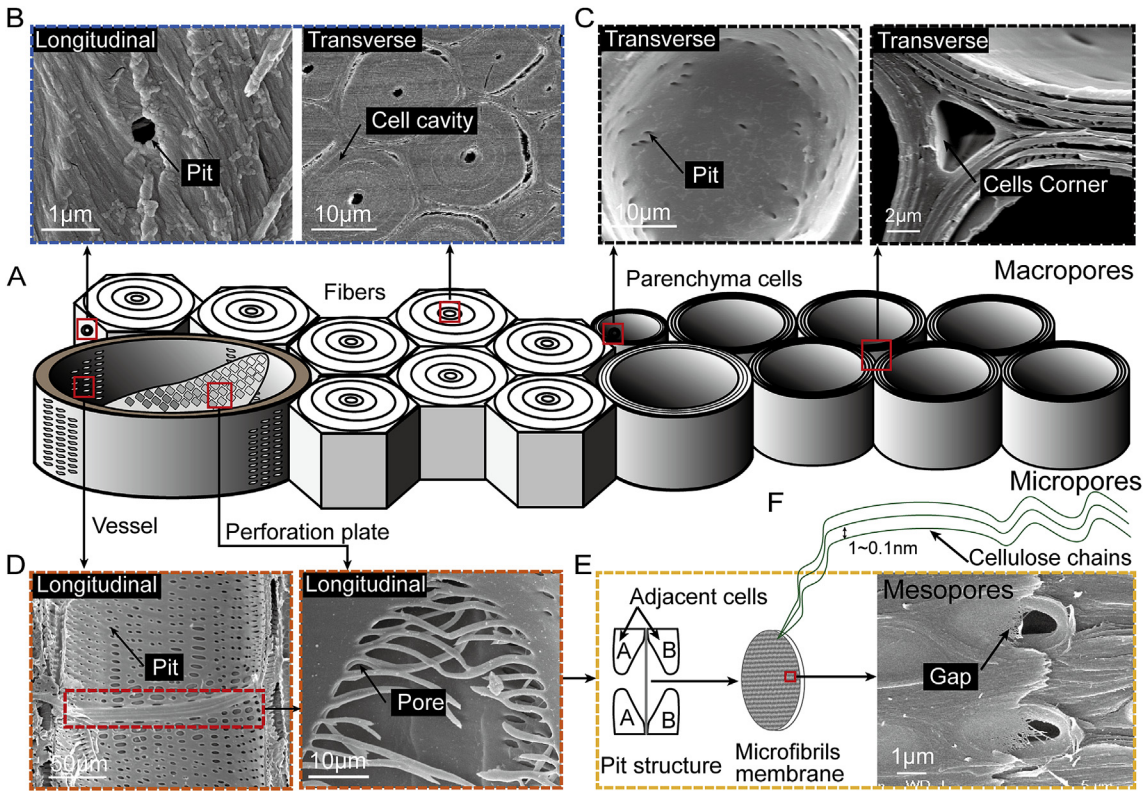

Fig. 6 – Pore structures in bamboo at multi-scale level. A. Schematic diagram of bamboo cells types, including fibers, parenchyma cells, and vessels (macropores); B. Cavities and pits in fibers; C. Cavities, pits and cell corner in parenchyma cells; D. pits in vessels and pores in perforated plate; E. The gap of microfibrils in the pit membrane (mesopores); F. the voids (1~0.1 nm) between cellulose chains (micropores).

average area of monolayer water molecules covering the bamboo surface (0.106 nm^2 was used) [32], and M (g/mol) is the molar mass of water.

The S values of the IB, MB, and OB layers were estimated to be 153, 143, and 132 m^2/g, respectively (Table 1); these values were consistent with the average value of 14 bamboo species (177 m^2/g) [12]. This indicates that the multi-scale structure of the bamboo itself can provide a natural channel for the preparation of charcoal, aerogel materials, and even solar energy-generating devices [33–36] via thermal or chemical activation.

4. Summary and conclusion

In this study, the hygroscopic behavior of bamboo with a gradient fiber structure was investigated via water vapor sorption isotherms fitted by the Haillwood–Horrobin (H–H) model. The effects of the chemical composition, gradient fiber structure, and mesopore structure were investigated. The main findings are summarized as follows.

(1) The bamboo was found to exhibit an increased equilibrium moisture content (EMC) and decreased hygroscopic hysteresis from the inner to the outer layer, which results from the gradient distribution of fibers and parenchyma cells along the thickness of the culm wall;

(2) Based on the H–H model, the hygroscopic mechanism of bamboo was determined as follows. The primary sites derived from amorphous cellulose and hemicellulose act in the low-humidity stage, while the mesopore provides a huge specific surface area, which helps condense water vapor in high-humidity environments.

(3) Based on the gradient fiber structure of bamboo and a numerical model, the contribution ratio of parenchyma cells and fibers to the overall hygroscopicity of bamboo was determined to be 13:5.

(4) The contribution of cellulose to hygroscopicity was found to become gradually higher than that of hemicellulose from the inner to the outer layer due to the increase of the amorphous area (–OH groups).

The structure–function relationships between the chemical composition, multi-scale structure, and hygroscopicity of bamboo determined in this study provide a theoretical basis for the bamboo drying and storage technology, as well as the processing and application of bamboo fiber-based composites.

Declaration of Competing Interest

The authors declare that they have no known competing financial interests or personal relationships that could have appeared to influence the work reported in this paper.

Acknowledgments

This work was financially supported by the National Natural Science Foundation of China (31770598). The authors would also like to thank Fujian Youzhu Technology Co., Ltd. for supplying the raw materials.

REFERENCES

[1] Wu Y, Zheng Y, Yang F, Yang L. Preparation process and characterization of mechanical properties of twisted bamboo spun fiber bundles. J Mater Res Technol 2021;14:2131–9. https://doi.org/10.1016/j.jmrt.2021.07.080.

[2] Deng J, Wei X, Zhou H, Wang G, Zhang S. Inspiration from table tennis racket: preparation of rubber-wood-bamboo laminated composite (RWBLC) and its response characteristics to cyclic perpendicular compressive load. Compos Struct 2020;241:112135. https://doi.org/10.1016/j.compstruct.2020.112135.

[3] Wei X, Zhou H, Chen F, Wang G. Bending flexibility of Moso Bamboo (*Phyllostachys edulis*) with functionally graded structure. Materials 2019;12:2007. https://doi.org/10.3390/ma12122007.

[4] Zhang Y, Huang X, Yu Y, Yu W. Effects of internal structure and chemical compositions on the hygroscopic property of bamboo fiber reinforced composites. Appl Surf Sci 2019;492:936–43. https://doi.org/10.1016/j.apsusc.2019.05.279.

[5] Wang X, Ren H, Zhao R, Cheng Q, Chen Y. FTIR and XPS spectroscopic studies of photodegradation of Moso bamboo (*Phyllostachys pubescens Mazel*). Spectrosc Spect Anal 2009;29:1864–7.

[6] Silva ECN, Walters MC, Paulino GH. Modeling bamboo as a functionally graded material:lessons for the analysis of affordable materials. J Mater Sci 2016;41:6991–7004. https://doi.org/10.1007/s10853-006-0232-3.

[7] Habibi MK, Samaei AT, Gheshlagh B, Lu J, Lu Y. Asymmetric flexural behavior from bamboo's functionally graded hierarchical structure: underlying mechanisms. Acta Biomater 2015;16:178–86. https://doi.org/10.1016/j.actbio.2015.01.038.

[8] Lin Q, Huang Y, Yu W. An in-depth study of molecular and supramolecular structures of bamboo cellulose upon heat treatment. Carbohydr Polym 2020;241:116412. https://doi.org/10.1016/j.carbpol.2020.116412.

[9] Choudhury D, Sahu JK, Sharma GD. Moisture sorption isotherms, heat of sorption and properties of sorbed water of raw bamboo (*Dendrocalamus longispathus*) shoots. Ind Crops Prod 2011;33(1):211–6. https://doi.org/10.1016/j.indcrop.2010.10.014.

[10] Chen Q, Wang G, Ma X, Chen M, Fei B. The effect of graded fibrous structure of bamboo (*Phyllostachys edulis*) on its water vapor sorption isotherms. Ind Crops Prod 2020;151:112467. https://doi.org/10.1016/j.indcrop.2020.112467.

[11] Krause JQ, Silva FDA, Ghavami K, Gomes ODFM, Filho RDT. On the influence of *Dendrocalamus giganteus* bamboo microstructure on its mechanical behavior. Constr Build Mater 2016;127:199–209. https://doi.org/10.1016/j.conbuildmat.2016.09.104.

[12] Zhang X, Li J, Yu Y, Wang H. Investigating the water vapor sorption behavior of bamboo with two sorption models. J Mater Sci 2018;53:8241–9. https://doi.org/10.1007/s10853-018-2166-y.

[13] Zauer M, Kretzschmar J, Großmann L, Pfriem A, Wagenführ A. Analysis of the pore-size distribution and fiber saturation point of native and thermally modified wood using differential scanning calorimetry. Wood Sci Technol 2014;48:177–93. https://doi.org/10.1007/s00226-013-0597-9.

[14] Wang T, Tian S, Li G, Li Sheng M, Ren W, Liu Q, et al. Experimental study of water vapor adsorption behaviors on shale. Fuel 2019;248:168–77. https://doi.org/10.1016/j.fuel.2019.03.029.

[15] Langmuir I. The adsorption of gases on plane surfaces of glass, mica and platinum. J Am Chem Soc 1918;40:1361–403. https://doi.org/10.1021/ja02242a004.

[16] Brunauer S, Emmett P, Teller E. Adsorption of gases in multimolecular layers. J Am Chem Soc 1938;60:309–19. https://doi.org/10.1021/ja01269a023.

[17] Haillwood AJ, Horrobin S. Absorption of water by polymers: analysis in terms of a simple model. Trans Faraday Soc 1946;42:84–102. https://doi.org/10.1021/ja02242a004.

[18] Depuydt DEC, Soete J, Asfaw YD, Wevers M, Ivens J, Vuure AW. Sorption behaviour of bamboo fibre reinforced composites, why do they retain their properties? Compos Part A Appl Sci Manuf 2019;119:48–60. https://doi.org/10.1016/j.compositesa.2019.01.020.

[19] Hill CAS, Norton A, Newman G. The water vapor sorption behavior of natural fibers. J Appl Polym Sci 2009;112(3):1524–37. https://doi.org/10.1002/app.29725.

[20] Papadopoulos AN, Avramidis S, Elustondo D. The sorption of water vapour by chemically modified softwood:analysis using various sorption models. Wood Sci Technol 2005;39(2):99–111. https://doi.org/10.1007/s00226-004-0272-2.

[21] Olek W, Majka J, Czajkowski Ł. Sorption isotherms of thermally modified wood. Holzforschung 2013;67(2):183–91. https://doi.org/10.1515/hf-2011-0260.

[22] Bedane AH, Xiao H, Eić M. Water vapor adsorption equilibria and mass transport in unmodified and modified cellulose fiber-based materials. Adsorption 2014;20:863–74. https://doi.org/10.1007/s10450-014-9628-6.

[23] Dixon PG, Ahvenainen P, Aijazi AN, Chen SH, Lin S, Augusciak PK, et al. Comparison of the structure and flexural properties of Moso, Guadua and Tre Gai bamboo. Constr Build Mater 2015;90(12):11–7. https://doi.org/10.1016/j.conbuildmat.2015.04.042.

[24] ASTM D1106-96(2013) standard test method for acid-insoluble lignin in wood. West Conshohocken, PA: ASTM International; 2013. www.astm.org.

[25] Zhang X, Huang H, Qing Y, Wang H, Li X. A comparison study on the characteristics of nanofibrils isolated from fibers and parenchyma cells in bamboo. Materials 2020;13(1):237. https://doi.org/10.3390/ma13010237.

[26] Yuan J, Chen Q, Fang C, Zhang S, Liu X, Fei B. Effect of chemical composition of bamboo fibers on water sorption. Cellulose 2021;28:7273–82. https://doi.org/10.1007/s10570-021-03988-3.

[27] Yuan J, Chen Q, Fei B. Investigation of the water vapor sorption behavior of bamboo fibers with different sizes. Eur J Wood Prod 2021;79:1131–9. https://doi.org/10.1007/s00107-020-01652-4.

[28] Zhang S, Liu R, Lian C, Luo J, Feng Y, Liu X, et al. Intercellular pathways in internodal metaxylem vessels of moso bamboo Phyllostachys edulis. IAWA J 2019;40(4):1–13. https://doi.org/10.1163/22941932-40190237.

[29] Monteiro S, Margem F, Braga F, Luz F, Simonassi T. Weibull analysis of the tensile strength dependence with fiber diameter of giant bamboo. J Mater Res Technol 2017;6(4):317–22. https://doi.org/10.1016/j.jmrt.2017.07.001.

[30] Papadopoulos A, Hill CAS. The sorption of water vapour by anhydride modified softwood. Wood Sci Technol 2003;37:221–31. https://doi.org/10.1163/22941932-40190237.

[31] Bratasz Ł, Kozłowska A, Kozłowski R. Analysis of water adsorption by wood using the Guggenheim-Anderson-de Boer equation. Eur J Wood Prod 2012;70:445–51. https://doi.org/10.1007/s00107-011-0571-x.

[32] Livingston H. The cross-sectional areas of molecules adsorbed on solid surfaces. J Colloid Interface Sci 1949;23:447–58. https://doi.org/10.1016/0095-8522(49)90043-4.
[33] Yan Y, Shi M, Wei Y, Zhao C, Carnie M, Yang R, et al. Process optimization for producing hierarchical porous bamboo-derived carbon materials with ultrahigh specific surface area for lithium-sulfur batteries. J Alloys Compd 2018;738:16–24. https://doi.org/10.1016/j.jallcom.2017.11.212.
[34] Chen C, Song J, Zhu S, Li Y, Kuang Y, Wan J, et al. Scalable and sustainable approach toward highly compressible, anisotropic, lamellar carbon sponge. Chem 2018;4(3):544–54. https://doi.org/10.1016/j.chempr.2017.12.028.
[35] Xu S, Chen C, Kuang Y, Song J, Gan W, Liu B, et al. Flexible lithium-CO_2 battery with ultrahigh capacity and stable cycling. Energy Environ Sci 2018;11(11):3231–7. https://doi.org/10.1039/C8EE01468J.
[36] Li T, Liu H, Zhao X, Chen G, Dai J, Pastel G, et al. Scalable and highly efficient mesoporous wood-based solar steam generation device: localized heat, rapid water transport. Adv Funct Mater 2018;28:1707134. https://doi.org/10.1002/adfm.201707134.